

Nanoscale

Accepted Manuscript



This is an *Accepted Manuscript*, which has been through the Royal Society of Chemistry peer review process and has been accepted for publication.

Accepted Manuscripts are published online shortly after acceptance, before technical editing, formatting and proof reading. Using this free service, authors can make their results available to the community, in citable form, before we publish the edited article. We will replace this *Accepted Manuscript* with the edited and formatted *Advance Article* as soon as it is available.

You can find more information about *Accepted Manuscripts* in the [Information for Authors](#).

Please note that technical editing may introduce minor changes to the text and/or graphics, which may alter content. The journal's standard [Terms & Conditions](#) and the [Ethical guidelines](#) still apply. In no event shall the Royal Society of Chemistry be held responsible for any errors or omissions in this *Accepted Manuscript* or any consequences arising from the use of any information it contains.

Submicron Polyacrolein Particles *in situ* Embedded with Upconversion Nanoparticles for Bioassay

A.N. Generalova,^{a,b,d} I.K. Kochneva,^a E.V. Khaydukov,^b V.A. Semchishen,^b A.E. Guller,^{c,f} A.V. Nechaev,^c A.B. Shekhter,^c V.P. Zubov,^{a,b} A.V. Zvyagin*^{d,f} and S.M. Deyev^{a,d}

^a M.M. Shemyakin & Yu.A. Ovchinnikov Institute of Bioorganic Chemistry of the Russian Academy of Sciences, 117997, Moscow, Russia

^b Institute on Laser and Information Technologies of the Russian Academy of Sciences, 140700, Shatura, Russia

^c I.M. Sechenov First Moscow State Medical University, 119992, Moscow, Russia;

^d N.I. Lobachevsky Nizhny Novgorod State University, 603950, Nizhny Novgorod, Russia;

^e M.V. Lomonosov Moscow University of Fine Chemical Technology, 119571 Moscow, Russia

^f MQ Biofocus Research Centre, Macquarie University, NSW 2109, Australia

*Corresponding author: Andrey Zvyagin, PhD, Associate Professor, e-mail: andrei.zvyagin@mq.edu.au

† Electronic Supplementary Information available: [SI 1, SI 2]. See DOI

Abstract

We report a new surface modification approach of upconversion nanoparticles (UCNPs) structured as an inorganic host NaYF₄ codoped with Yb³⁺ and Er³⁺ based on their encapsulation at a two-stage process of precipitation polymerization of acrolein under alkaline conditions in the presence of UCNPs. The use of tetramethylammonium hydroxide both as an initiator of the acrolein polymerization and agent for the UCNP hydrophilization made it possible to increase the polyacrolein yield up to 90%. This approach enabled facile, lossless embedment of UCNPs into the polymer particles suitable for bioassay. These particles are readily dispersible in aqueous and physiological buffers, exhibiting excellent photoluminescent properties, chemical stability, and allowed control of the particle diameters. The feasibility of as-produced photoluminescent polymer particles mean-sized 260 nm for *in vivo* optical whole-animal imaging was also demonstrated using a home-built epi-luminescence imaging system.

Key words: polyacrolein particles, upconversion nanoparticles, *in situ* encapsulation, precipitation polymerization, bioimaging.

Introduction

The last decade has seen a productive confluence of Life Sciences and Nanotechnology. In particular, photoluminescent (PL) nanomaterials, such as quantum dots,¹ gold nanoparticles,² metal-

ligand complexes³ and fluorescent nanodiamonds⁴ provide means for imaging biomolecular processes in a broad physiological context. The exceptional photophysical properties of these nanoparticles (NPs) push the sensitivity limit to the single biomolecule level, while the well-developed surface of these NPs represents a flexible platform, where various surface moieties can be attached to, enabling to dock targeting and/or therapeutic biomolecules. These biomolecules and NPs are pieced together to form a targeting hybrid nanoassembly with diagnostic capabilities, whereas the attachment of therapeutic cargo enables treatment of these targeted cells or biological tissues.

Lanthanide-doped upconversion nanoparticles (UCNPs) represent one of the most promising type of these PL nanomaterials. UCNPs are characterised by sharp absorption and emission lines, high conversion efficiency,⁵ long lifetimes, low reported cytotoxicity,⁶ negligible photobleaching,⁷ and high spatial-temporal resolution during bioimaging.⁸ The efficient conversion of near-infrared (NIR) excitation at the wavelength of 980 nm into the shorter-wavelength infrared and visible spectral range emission (known as “upconversion”) represents its most acclaimed property. The near-infrared excitation band of UCNPs entails two additional useful properties. Firstly, the excitation of intrinsic tissue fluorescence, known as autofluorescence, is almost negligible⁹; secondly, the excitation light penetration in biological tissue is greater in comparison with visible light, up to one centimeter, because the excitation band falls into the so-called biological tissue transparency window.^{10,11}

In most cases, UCNP is composed of a host matrix doped with sensitizer and activator rear-earth ions. The most effective matrix for the NIR-to-visible or the shorter-wavelength NIR upconversion has been reported¹² to be a hexagonal phase (β -phase) NaYF₄ crystal characterised by the low phonon energy. The sensitizer (Yb³⁺) and activator (Er³⁺ and/or Tm³⁺) are doped in the host matrix in relatively low concentrations, usually 20 mol% and (2 and/or 0.5 mol%), respectively. Typically, these UCNPs are synthesized in organic solvents, resulting in UCNPs stabilized with hydrophobic oleate ligands. They are dispersible only in nonpolar organic solvents and aggregate in aqueous solutions and physiological buffers, which limits their biomedical application scope. Surface hydrophilization of UCNPs, therefore, represents an essential prerequisite for grafting UCNP surface with reactive functional moieties suitable for conjugation with biomolecules.

A number of surface modification approaches have been reported, including: (i) ligand oxidation reaction;¹³ (ii) ligand exchange reaction;¹⁴ (iii) intercalation using amphiphilic polymers;¹⁵ (iv) cross-linked polymer coating;¹⁶ (v) layer-by-layer self-assembly;¹⁷ (vi) host-guest self-assembly;¹⁸ (vii) encapsulation of NPs in silica.¹⁹ As a result, as-synthesized hydrophobic PL NPs are rendered dispersible in aqueous media, allowing further bioconjugation with biomolecules, while preserving their photoluminescent properties.²⁰ However, most of these approaches usually result in the

formation of a loose protective shell around a UCNP, unable to shield the UCNP surface from solvent molecules, including ions of buffer salts, which can penetrate and damage the UCNP surface resulting in fluorescence quenching.²⁰

Embedment of UCNPs into polymer particles obtained by heterogeneous polymerization, while transferring to aqueous media, represents a promising approach of tight shielding of the UCNPs by the formation of a solid polymer shell impenetrable to small solvent molecules. To the best of our knowledge, such approach has not been reported for UCNPs. At the same time, polymer particle hosts have been employed for encapsulation of such inorganic fillers as quantum dots,²¹ iron oxides,²² metal-ligand complexes,²³ *etc.* Usually, these fillers were encapsulated either into preformed polymer particles swelled in appropriate solvent,²⁴ or in the course of the polymerization procedure.²⁵ Although the preformed polymers provide adequate isolation of inorganic fillers from physiological environment, the fillers are not securely anchored and can escape the polymer host, if its structural properties, *e.g.* porosity, change in response to the environmental changes.²⁴

In order to address the problem of the filler retention in the polymer host, we propose the following new synthesis concept: the polymerization itself is initiated by the fillers, in our case, hydrophilized upconversion nanoparticles, which are introduced at the stage of polymerization. As a result, UCNP forms bonds with the polymer matrix during its *in situ* formation, eventually yielding a hybrid water-dispersible sub-micron polymer particle containing a UCNPs well secluded from aqueous environment, but capable of interfacing with biomolecules. The challenge of *in situ* embedding of UCNPs into a polymer matrix lies in the design of the method providing chemical compatibility between the UCNP and polymer chains while protecting the optical properties from quenching agents, photobleaching, and effects of solvent polarity, pH, and ionic strength.

Acrolein was as the monomer, giving rise to polymer particles readily dispersible in water, with variable particle diameters and with aldehyde groups on the surface.²⁶ These groups easily form Schiff's base with primary amine groups of biomolecules under mild conditions. We have previously reported two-stage precipitation polymerization of acrolein in aqueous media under alkaline conditions.²⁴ This reaction was modified aiming at the encapsulation of UCNPs into polyacrolein (PA) particles and chemical compatibility between the UCNPs and polymer chains. This was realized by hydrophilization of UCNPs using tetramethylammonium hydroxide (TMAH), which can promote the transfer from an organic to an aqueous media.²⁷ The base strength of TMAH is close to alkali that makes it possible to use TMAH as an initiator of acrolein polymerization.

In this paper, we report on a new synthesis of polymer particles embedded with UCNPs in the course of the polymerization. The use of TMAH both as hydrophilizing agent of UCNPs and initiator of acrolein polymerization in the presence of UCNPs resulted in the formation of uniform bright PL polymer particles whose diameters was controllable in the broad range. The PL properties

of the UCNPs were protected from quenching agents of the environmental surroundings in the secluded polymer matrix whose colloidal chemical properties were suitable for theranostics applications, one example of which was demonstrated by whole-animal imaging.

Results and discussion

1. Synthesis of upconversion nanoparticles

The UCNPs ($\text{NaYF}_4:\text{Yb}^{3+}, \text{Er}^{3+}$) were synthesized by a modified solvothermal method, as described in Ref.¹⁵ and imaged by TEM (see Fig. 1). As-synthesised UCNP mean-size was evaluated as 41 ± 3 nm, and featured the most favorable for the energy transfer upconversion process hexagonal crystal phase.²⁸

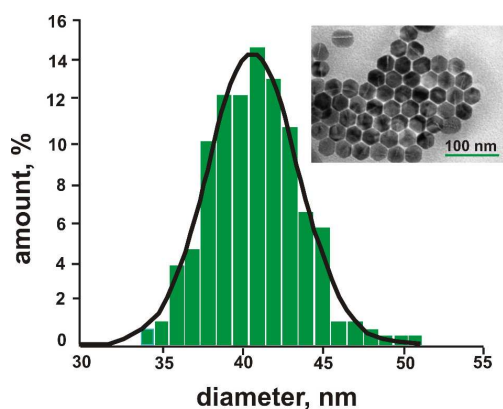


Figure 1. Size distribution histogram and TEM image of as-synthesised $\text{NaYF}_4:\text{Yb}^{3+}/\text{Er}^{3+}$ nanoparticles.

The as-synthesized UCNPs were capped with hydrophobic oleate ligands and hence neither miscible with water, nor suitable for immediate bioconjugation with biomolecules.

2. Synthesis of polymer particles embedded with UCNP in the course of polymerization

2.1. Design of polymerization method

Recently, we have reported on the production and characterisation of preformed polyacrolein (PA) particles served as a matrix for the encapsulation of the fillers, i.e. quantum dots.²⁴ Despite their promising colloidal and photoluminescent properties suitable for bioimaging, they showed propensity for desorption of quantum dots from the PA particles and concomitant degradation of the PL efficiency. In order to avoid the desorption of the filler, we developed approach, which was realized by introduction of the filler, upconversion nanoparticles, in the course of acrolein polymerization, as detailed in “Materials and Methods”. The reaction scheme is presented in Fig. 2A.

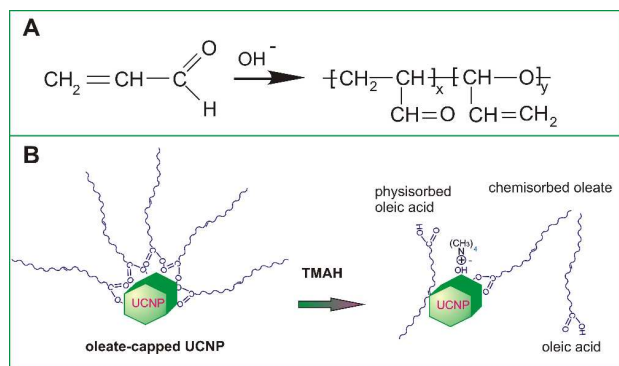


Figure 2. Schematic formula of acrolein polymerization under alkaline conditions (A); Schematic diagram of UCNP hydrophilization by the tetramethylammonium hydroxide (B).

The formation of polyacrolein particles can be briefly described, as follows. Acrolein is a partially water-soluble monomer (about 20% v.), whereas polyacrolein particles are not soluble in water. At the 1st polymerization stage, the initial mixture contains dispersion media (water), droplets of monomer (acrolein) and dissolved monomer. The polymerization reaction begins, when an initiator (alkali) is added and OH^- of alkali initiates the growth of polymer chains of dissolved acrolein. When the chains reach a critical length, their decreased solubility in water makes them unstable in solution, and they begin to aggregate into small particles, which serve as seeds. These seed particles are coated with short polyacrolein oligomers, which keep them suspended in the solution. Depletion of the water-phase acrolein causes acrolein diffusion from the droplets into the seeds driven by the higher solubility of acrolein inside the particle than in water, as well as formation of new oligomers that can either diffuse or adsorb on the seed particles. The polymerization reaction then takes place inside the particles and proceeds until all monomer and short chain oligomers are consumed. The typical diameter of thus prepared polyacrolein particles is about 600 nm. At the second stage of polymerization, the particle colloidal-chemical stability is increased by means of cross-linking of the residual $\text{C}=\text{C}$ bonds.

In order to introduce the filler, i.e. UCNPs, into the PA polymer at the 1st polymerization stage, it has to be sufficiently hydrophilic to facilitate its transport through the water phase from the monomer droplets to the growing seed particles. The surface of the as-synthesized UCNPs, however, is strongly hydrophobic due to the coordination with oleate ligands, which precludes its solubility in a variety of monomers and solvents. Our initial experiments proved that, indeed, as-synthesized UCNPs were not miscible with acrolein. We developed a new approach, which satisfied both the conditions for the encapsulation of UCNP into polyacrolein particles and the chemical compatibility between UCNP and the polymer chains. To this aim, UCNPs were hydrophilized by TMAH, making possible their transfer from organic solvent to aqueous media,²⁷ whereby the oleate ligands were partially displaced from the UCNP surface. In addition, the base strength of TMAH

was close to that of alkali usually employed in the polymerization reaction that makes it possible to use TMAH as initiator of acrolein polymerization.

The oleate ligands were chemically adsorbed on the UCNPs through the coordination between the COO^- group and the lanthanide ions on the surface.²⁹ As reported in the literature,³⁰ partial removal of oleate ligands from the UCNPs surface (as demonstrated using magnetite NPs) reduced the hydrophobicity and made it possible to prepare the polymer particles with controllable content of nanoparticles. In our case, we hydrophilized the oleate-capped UCNPs by applying a facile base reaction with TMAH,²⁹ which resulted in the partial release of oleic acid from the surface. In order to confirm this reaction outcome, we acquired and analysed Fourier-transform infrared (FTIR) spectra of UCNPs, UCNPs hydrophilised with TMAH, followed by further purification with water (Fig. 3B), and with water-acrolein mixture (20:1 vol) (Fig. 3C). Water-acrolein mixture was used since oleic acid being almost insoluble in water can remain in samples after purification.

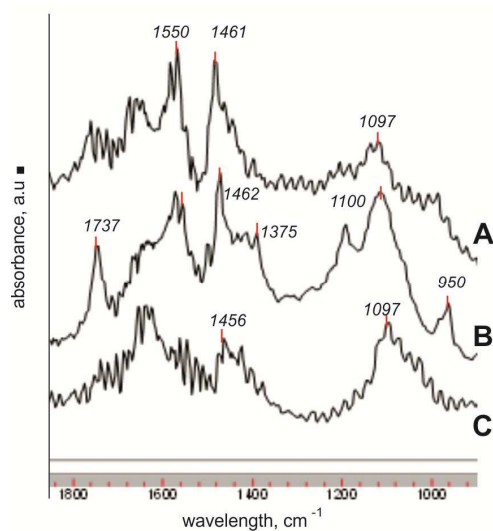


Figure 3. FTIR-spectra of the UCNPs sample: (A) in dry powder form; (B) hydrophilized with tetramethylammonium hydroxide, (C) purified with water-acrolein (20:1 vol) mixture.

The spectra of UCNPs (Fig. 3A) and UCNPs+TMAH purified with water (Fig. 3B) are almost identical within two bands: 1461 and 1545 cm^{-1} , which are attributed to the asymmetric (δ_s) and the symmetric $-\text{COO}-$ (δ_{as}) stretches of oleic acid, respectively.³¹ A strong stretching vibration of $-\text{C}=\text{O}$ assigned to oleic acid appears at 1737 cm^{-1} in the sample treated with TMAH and purified with water (Fig. 3B). However, this characteristic band of the $\text{C}=\text{O}$ stretch practically disappears in the sample C spectrum (Fig. 3C), indicating the removal of the outer layer of oleic acid after the purification with water-acrolein mixture.³⁰ In addition, the removal of oleic acid is corroborated by the disappearance of a peak at 1545 cm^{-1} and decrease of the stretching band at 1461 cm^{-1} .

Based on this analysis, our interpretation of the TMAH-based reaction is schematically presented in Fig. 2B. Oleic acid chemically adsorbed on the as-synthesised UCNPs surface was partially

displaced with TMAH, facilitating UCNP hydrophilization and its transferal to aqueous media. It was likely that the hydrophilized UCNPs still contained oleic acid moieties, which were physisorbed by intermolecular forces (van-der-waals, hydrophobic, hydrogen bond formation) on the UCNP surface. These moieties were resilient to washing with water, but removable with organic solvents.

We found that TMAH initiated the acrolein polymerization in the absence of UCNPs with the polymer yield in excess of 90% (see Fig. 5) in comparison with that of alkali measured as 45%.²⁴ TMAH seemed to cause the formation of the more effective carbanion of acrolein at the chain propagation reaction. In aqueous media, an ion $N^+(CH_3)_4$ can support the presence of free ions (these free ions promote polymerization unlike contact pairs of ions, which inhibit the polymerization³²) owing to steric hindrance more efficiently than Na^+ in alkali, thus causing the higher monomer conversion, and subsequently higher polymer yield.

Since TMAH was found to be capable to initiate the high-yield polymerization reaction, it was anticipated that TMAH-surface-modified UCNPs would efficiently initiate the polymerization reaction. In order to demonstrate this reaction mechanism, we synthesized polyacrolein particles with addition of UCNPs in the range of concentration (C_{UCNPs}) from 0.1 to 1.5 % wt. calculated with respect to the monomer (Fig. 4A).

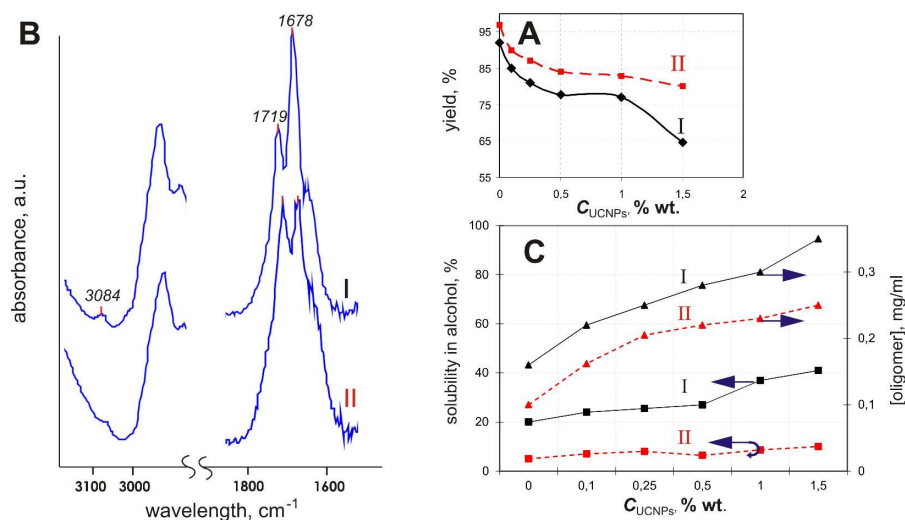


Figure 4. Polyacrolein yield versus UCNP concentrations in the course of polymerization (A); FTIR spectra of polyacrolein particles after the first and second stage of polymerization in the presence of UCNPs (B); Solubility of polyacrolein particles in alcohol and oligomer concentration versus concentration of UCNPs (C). (I designates the polymerization under alkaline conditions; II designates the radical cross-linking of the residual $C=C$ bonds)

Indeed, TMAH as a part of hydrophilized UCNPs resulted in the high polymer yields for all tested C_{UCNPs} , as shown in Fig. 4A. The polymer yield was found to decrease versus the C_{UCNP} . We speculate TMAH displaced the oleate ligands from the UCNP surface and the increase of C_{UCNP} caused the depletion of OH^- ions in dispersion medium, which promoted the propagation of

polymerization, so that the polymer yield was decreased as C_{UCNPs} increased. In the FTIR spectrum of UCNP-TMAH (Fig. 3B), a single band at 950 cm^{-1} attributed to the asymmetric C–N stretch³³ is observable, in contrast with the dry UCNP powder spectrum (Fig. 3A). Moreover, a new peak at 1375 cm^{-1} and a 1100 cm^{-1} peak increase, which are characteristic for the deformation vibration of O–H,³⁴ suggest the TMAH adsorption on the UCNP surface, causing the polymer yield decrease.

Thus, the proposed method assisted by UCNPs provides a well-controlled synthesis of PA particles with a high polymer yield, these assemblies are hereafter abbreviated as PA-UCNP.

2.2. 2nd polymerization stage

At the 2nd polymerization stage, the radical initiator ($\text{K}_2\text{S}_2\text{O}_8$) caused the polymerization of the residual double bonds of acrolein. Fig. 4 presents the FTIR spectra of polyacrolein particles after the 1st and 2nd polymerization stages in the presence of the hydrophilized UCNPs. The FTIR spectrum exhibited the change in relative intensity of peaks at 1719 cm^{-1} attributed to C=O of aldehyde group and 1678 cm^{-1} assigned to $\text{C}=\text{C}$.³⁵ The reduction of peak at 1678 cm^{-1} indicated the decrease of the terminal double bond relative to number of aldehyde groups. Besides, no vibration band at 3080 cm^{-1} attributed to $=\text{CH}_2$ ³⁵ was observable in the spectra of the sample after the second stage (Fig. 4B). Note, the crosslinking of residual double bonds in polymerization provided the increase of the polymer yield and chemical stability. The polymer particles became practically insoluble in alcohol and concentration of water-soluble oligomers as a typical side-product of acrolein polymerization formed during this synthesis decreased (Fig. 4C).

However, it is worth noting that the chemical stability of the resultant particles decreased versus the UCNP concentration, as shown in Fig. 4C. This effect was apparently related to the steric hindrances of the growing oligomer chain to access the active center (OH^\cdot) partially adsorbed on the UCNP surface. It arrested the growth of the water-soluble short chain oligomers, leading to their diffusion to dispersion medium. As a result, PA particles became loose, allowing infiltration of alcohol molecules.

3. Characterization of PA particles synthesized in the presence of UCNPs

The obtained particles remained colloidally stable for at least 6 months, and were unaffected by electrolytes (0.15 M NaCl and other physiological buffers).

It is important to note that functional (aldehyde) groups of the hybrid PA particles are convenient for their coupling with biomolecules, paving way for a broad range of imaging and targeted delivery applications. Owing to the nonporous character of the PA matrix,³⁶ only aldehyde groups on the PA particle surfaces participate in the immobilization of biologically active molecules. We found that the concentration of surface aldehyde groups per 1-g of the polymer particles was increased versus the C_{UCNPs} after the 2nd polymerization stage, as shown in Fig. 5A.

3.1. Particle diameters

The use of TMAH as the initiator of the polymerization provided the formation of pristine polymer particles with the diameter (d) larger (Fig. 5A) than that obtained in the course of the alkali-induced polymerization of acrolein ($d = 620$ nm), as previously reported in Ref. ²⁴. It was explained by the fewer nucleation centers generated in the case of TMAH than these in the case of alkali, provided the concentrations TMAH and alkali were equal. We speculate the early-stage initiation was accompanied by the salvation of counterion, which, probably, prevailed in the case of an alkali counterion Na^+ ³². The decrease of the nucleation centers gave rise to the increase of d , in the case of TMAH.

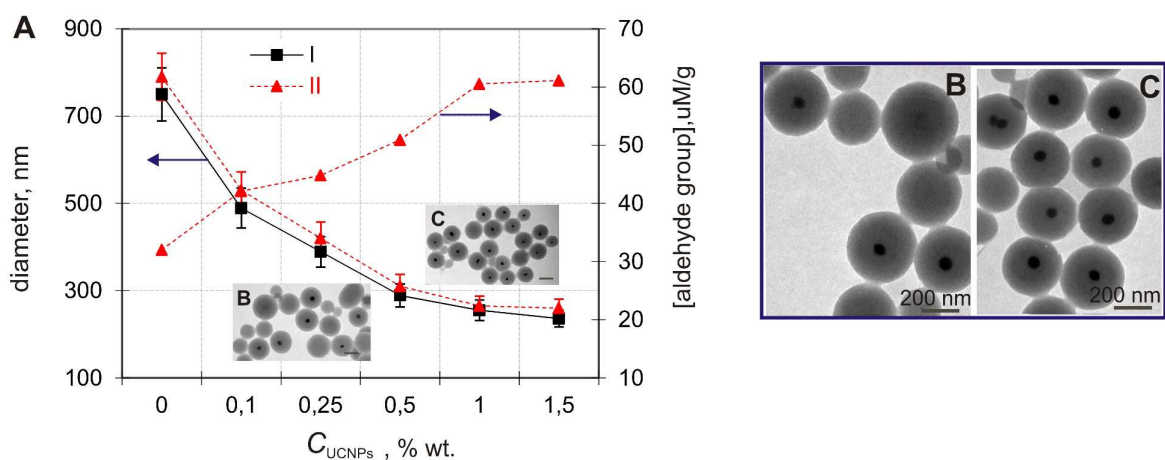


Figure 5. Diameters of polyacrolein particles impregnated with UCNPs versus UCNP concentration (A); TEM images of polyacrolein particles obtained in the presence of UCNPs: 0.25 %wt. mean-diameter, 400 nm (B); 1.5% wt. mean-diameter, 260 nm (C). Scale bar, 200 nm. (I designates polymerization under alkaline conditions; II designates radical cross-linking of the residual $\text{C}=\text{C}$ bonds).

d of the PA-UCNPs particles depended on the concentration of the inorganic NPs and varied from 500 to 260 nm, as it was measured by using a method of dynamic light scattering (Fig. 5A). It is worthy to note that the higher the concentration of UCNP in the polymerization initial mixture, the smaller the particles formed at the 1st polymerization stage. d remained practically unchanged at the 2nd polymerization stage (Fig. 5A). This observation can be explained in the terms of the PA particle stabilization in the course of the polymerization. As described earlier, the short-chain oligomers prevented aggregation of the PA particles. At the same time, their surface activity was insufficient to significantly decrease the diameter, since the reduction of the dynamic surface tension at the water-air interface by the oligomers was in excess of 60 mN/m, falling short of the value of 30 mN/m achievable with effective surfactants.³⁷ We refer to the Supplementary Information section 1 (SI-1) for more details. Also, the oligomers were likely to desorb from the PA particle surface to the dispersion media. The decrease of d was also due to the influence of another

surface active moiety, oleate ligand, physisorbed on the UCNP surface after the hydrophilization treatment with TMAH. Being a surfactant, oleate ligands can adsorb on the surface during the synthesis of PA particles thus reducing d . At the UCNP concentration greater than 0.5 % wt., the effect of oleic acid diminished, and the d variation halted.

3.2. Structural and photoluminescent properties of hybrid PA-UCNPs

The UCNP-assisted acrolein polymerization can be classified as a template polymerization, which is characterized by specific interactions between the template, *i.e.* UCNP, and the growing polymer chains. The oligomer complexation with the template occurs in solution via intermolecular forces, when the oligomers reach a critical length. Then the oligomers continue to propagate along the template by sourcing monomer molecules from the surrounding media.³⁸

TEM images of PA-UCNP particles synthesized *in situ* are shown in Fig.5. UCNPs were seen buried at the center of the polymer host, thus confirming the template role of UCNP, with a polymer shell formed around the UCNP core. Pristine coreless PA particles were also formed. The proportion of the PA-UCNP to pristine PA particles showed a clear tendency to grow versus the C_{UCNPs} in the range from 0 to 1% wt., as graphed in Fig. 5C. This graph plateaus at 1% wt., the proportion of the pristine PA particle remained constant, while the PA-UCNPs occasionally featured more than two UCNP cores. We speculate that both precipitation and template polymerization mechanisms participated in the formation of PA-UCNPs.

It is worth noting that all UCNPs appeared to be embedded in PA particles, as suggested by two observations: 1. TEM imaging revealed no individual UCNPs but embedded into PA particles; 2. no photoluminescence of the supernatants after the centrifugation of PA-UCNPs particles was detected, hence the supernatants contained no stand-alone UCNPs.

Several comments on the PL properties of the hybrid PA-UCNP assemblies are now in order. The susceptibility of UCNPs to environmental effects is notorious and addressed in many reports.¹⁰⁻¹² Oleic acid ligands coordinated to the UCNP surface were found to reduce this susceptibility and protect the UCNP emitting state from environmental surroundings, which ushered the UCNP uptake in Life Sciences²⁸. The TMAH-mediated replacement of the oleic ligands with PA polymer preserved the high PL efficiency of the oleic-coordinated UCNP. In particular, an intensity ratio of the characteristic green and red spectral bands of NaYF₄:Yb,Er were reported to be a sensitive indicator of the PL emission state variation due to environmental effects.²⁹ As can be inferred from the PL spectra of UCNPs and PA-UCNPs particles at the 1st and 2nd production stages (Fig. 6A), the green-to-red emission ratio calculated for all C_{UCNPs} remained unaltered. Based on this result, we assume passivation of the UCNP quenching surface defects by the polymer shell occupying vacant coordinate sites on the UCNP surface.²⁸

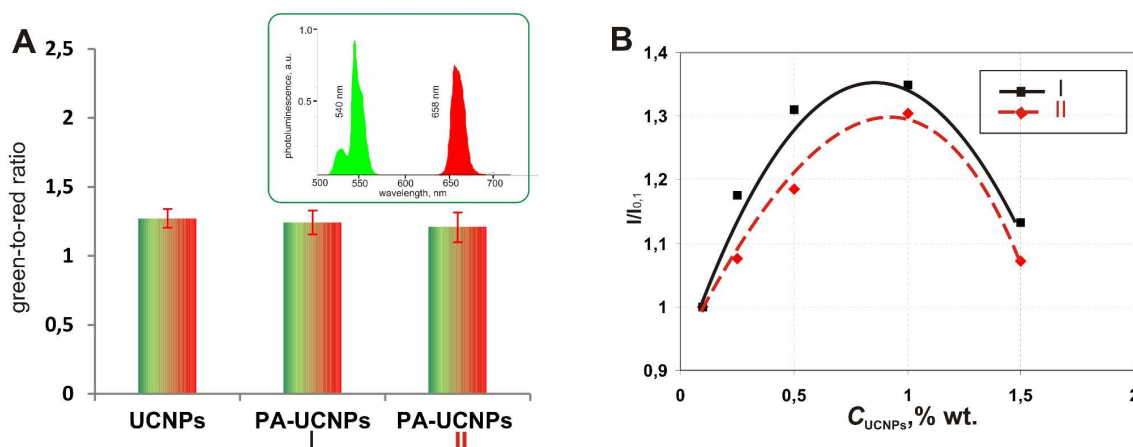


Figure 6. The green-to-red emission ratio from PL spectra of UCNP and polyacrolein particles impregnated with UCNP obtained under the laser excitation at wavelength 975 nm. Excitation intensity, 10 W/cm² (A); Insert represents PL spectrum of UCNP in chloroform. A plot of the PL intensity, I normalised to the reference intensity $I_{0.1}$ versus the UCNP concentration. $I_{0.1}$ is defined as the PL intensity at 0.1 % wt. UCNP (B). (I designates polymerization under alkaline conditions; II designates radical cross-linking of the residual C=C bonds).

In order to analyze the PL dependence on the C_{UCNP} in the polymerisation initial mixture), we plotted the PL signal intensity at 545 nm versus C_{UCNP} (Fig. 6B). The maximum PL efficiency occurred at $C_{UCNP} = 1\%$ wt. with respect to the monomer. The PL decrease at $1\% \text{ wt.} < C_{UCNP} < 1.5\% \text{ wt.}$ can be explained by the formation of UCNP aggregates inside the PA particles. In this case, a poor polymer shell was formed on the surface of UCNP in their contact area, resulting in the insufficient surface passivation, and hence the PL degradation.²⁸ As one can see from Fig. 6B, the PL signal changed slightly after the 2nd polymerization stage. The reason behind this variation is unclear and warrants further study.

4. Application of PA-UCNP particles for optical bioimaging

In order to demonstrate the feasibility of application of photoluminescent polymer particles in Theranostics, we carried out an *in vivo* whole-animal imaging experiments using PA-UCNP intravenous injection. Preliminary MTT assay for evaluation of PA-UCNPs and UCNP-TMAH cytotoxicity demonstrated low cytotoxic effects performed on linear keratinocytes HaCaT (see SI 2, Figure S2). We designed an epi-luminescence imaging system equipped with a raster-scanning laser excitation source to visualize PA-UCNP distribution in a live mouse (see Fig.7A). The laser light was projected onto the animal surface and emitted photoluminescence was collected from the same side with a camera lens (f-number 0.95).³⁹ The raster scanning was implemented with a collimated beam of a continuous-wave semiconductor laser operated at wavelength 975 nm, redirected off of fast galvanometer scanning mirror units (Miniscan-07, Raylase®, Germany). The elicited PL signal was recorded by an electron-multiplication (EM) CCD camera (Falcon, Raptor Photonics®, Ireland). The position of the camera was adjusted so as to make its matrix and the top surface of the

mouse lie in the optically conjugate planes. Rejection spectral filters were used to suppress the excitation signal in the detection path.

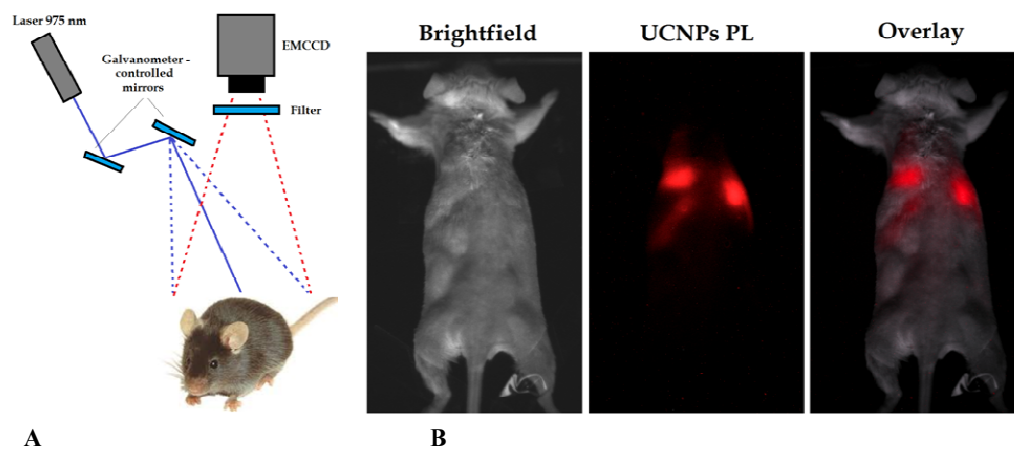


Figure 7. Schematic rendering of the epi-luminescence imaging system (A). *In vivo* photoluminescence imaging of a live mouse, past 1-hour intravenous injection of PA-UCNPs. Left: a bright-field image; centre: PL image; right: an overlay of the bright-field and PL images (B).

In order to demonstrate visualization of the biodistribution of PA-UCNP particles *in vivo*, 0.5 mg of PA-UCNPs ($C_{\text{UCNP}} = 1\%$ wt.) suspended in 0.1 mL of phosphate buffer saline (or blood plasma) was injected in the animal tail vein. No acute systemic toxicity and allergic reactions were observed. The following sequence of pharmacokinetic events was observed (see Fig.7B). A rapidly vanishing signal at the venipuncture site was noticeable immediately after the injection. In 5-10 min post-injection, a bright signal in the projection of the lungs (both from chest and back sides) was clearly detectable in 10 investigated animals. Then PL was redistributed towards the projections of the spleen and liver, reached its maximum in 60 - 80 min, while it virtually disappeared in the lungs. Furthermore, a weak PL signal in projection of bowel and pelvic organs of animals was observed 40-60 min post-injection. Apparently, no PL signal was detected in animals injected with pristine PAs.

It was also possible to perform informative PL *ex vivo* imaging of organ tissue slices using our epi-luminescence imaging system. PA-UCNPs particles were found immobilised in tissue sections of liver, spleen, lungs and kidney (see SI-2, Table S2), with the maximum accumulation observed in the liver and spleen. In addition, PA-UCNPs were observed in the lungs with a trend of the increasing local concentration at the areas of partial atelectasis. In the kidney, the PL clusters were hardly detectable localized mainly near the proximal convoluted renal tubules.

According to the histological data of the organ tissue slices harvested and processed post-injection PA-UCNPs, pathological changes after were minor or absent. In particular, moderate blood congestion was revealed in the central and triad veins in the liver. In lungs, small lymphocyte and macrophage infiltrates with individual neutrophils and plasma cells were found in the vicinity of the

large bronchi and blood vessels. In kidney and spleen, the tissue structure was found normal (see SI-2, Table S2).

Thus, polyacrolein particles *in situ* embedded with upconversion nanoparticles have great potential as bioimaging probes well suited for fluorescence visualization in whole animals.

Experimental

1. Materials

Acrolein purchased from Fluka (Germany) was distilled three times at atmospheric pressure and the fraction with boiling point of 56°C, $\rho_4^{20} = 0.806 \text{ g/cm}^3$, $n_D^{20} = 1.40$ was used. Polymer yield was measured gravimetrically.

The following materials were purchased from Sigma-Aldrich (USA), and used without further purification: potassium persulfate, sodium hydroxide, sodium chloride, phosphate buffered saline (PBS), sodium azide, tetramethylammonium hydroxide pentahydrate (TMAH), p-nitrophenylhydrazine. Ethanol, hexane, chloroform were of analytical grade and purchased from Sigma-Aldrich.

2. Methods

The size of particles was measured by Coulter N4-MD submicron particle analyzer (Coultronics, France). Optical characteristics were measured using Beckman DU-70 spectrophotometer (Beckman, Germany). Spectra of fluorescence were recorded by spectrofluorometer Fluorolog (Horiba Jobin Yvon, France). Photoluminescence of histological sections were registered by fluorescent microscope, as previously reported in Ref.¹⁵

2.1. Polymerization of acrolein in the presence of UCNPs. Polymerization of acrolein was carried out, as reported previously in Ref.²⁴ with some modifications. In the beginning, dispersions with varying concentrations of UCNPs in TMAH were obtained: 10, 25, 50, 100 or 150 μl of UCNP dispersion (20 mg/ml) in chloroform was added dropwise to a 1-ml of 1% aqueous solution of TMAH and two immiscible phases were thoroughly shaken and sonicated for 15 min. UCNPs were transferred from one phase to another, chloroform was evaporated. Then, freshly distilled acrolein 0.2 ml was placed in a three-necked reaction flask containing water (monomer:water = 1:20 v/v) under stirring. One of the aforementioned UCNP dispersion in TMAH was added dropwise under stirring. After 3 h of stirring at room temperature, water insoluble polymer particles were formed. Then, the reaction mixture was deoxygenated by purging with N_2 for 30 min and $\text{K}_2\text{S}_2\text{O}_8$ (2% wt in respect to monomer) was added to increase the chemical stability of the obtained polymer particles. The mixture was kept at 70°C under N_2 and stirred for 3 h. The procedure was repeated for all concentrations of UCNPs in TMAH.

2.2. Measurement of the aldehyde group concentration. The aldehyde group concentration was measured by using *p*-nitrophenylhydrazine (NPH) in alcohol/phosphate buffer pH 5.3 as we reported previously in Ref.²⁴. The supernatants of the mixture containing 1 mL of NPH and 100 μ L 5% wt. polymer particle dispersion after the preparation and after incubation for 8 h were collected and analyzed using a spectrophotometer Beckman DU-70 at wavelength 392 nm. The aldehyde group concentration was calculated as the concentration of NPH that have reacted with aldehyde groups.

2.3. Measurement of the acrolein oligomer concentration. Polyacrolein dispersion was centrifuged and supernatant containing acrolein oligomers was measured using the spectrophotometer Beckman DU-70 at wavelength 273 nm, as we reported previously in Ref.²⁴. The acrolein oligomer concentration was calculated using the calibration graph of optical absorption of dry oligomer dissolved in water.

2.4. Transmission electron microscopy (TEM). The UCNP and polyacrolein particles containing UCNPs were diluted by hexane and water, respectively, then sonicated and dropcasted onto a thin bar 300-mesh copper TEM grids, coated with 0.3% pioloform. After overnight drying in a desiccator at room temperature, the grids were imaged using a Philips CM10 TEM (Philips, Eindhoven, The Netherlands).

2.5. Sample preparation of UCNPs in TMAH for FTIR Spectroscopy. The UCNP dispersions in TMAH were prepared as described in 2.1. To remove an excess of TMAH, one sample of the aqueous UCNPs was purified three times with water (consecutive centrifugation at 13400 rpm for 10 min – redispersion steps). The pellet was air-dried. Another sample at the same concentration of UCNPs was purified three times in the same manner with water-acrolein mixture (1:30, v/v) at 0°C to avoid oligomer formation. The pellet was air-dried.

2.6. Fourier-transform infrared (FTIR) spectroscopy. Pure UCNPs was thoroughly ground and then pressed with KBr to form a tablet. The air-dried samples of UCNP modified with TMAH: purified with water and with water-acrolein, as well as polymer particles were dried using a Savant SpeedVac Concentrator (France), then ground and pressed with KBr to form a tablet. FTIR spectra were recorded using an FTIR spectrophotometer (Varian 3100, USA).

2.7. Mice for in vivo imaging, microscopy and morphological study. Preliminary animal imaging experiments were performed in male BALB/c mice weighing 20-25 g to examine biodistribution of these particles after a single intravenous injection. The study was carried out with the permission of the Ethics Committee of I.M. Sechenov First Moscow State Medical University. Anaesthesia was performed by using the mixture of Zoletil (5.0 mg/kg), and 10 μ L of 2% Rometar solution. The anaesthetic cocktail was administered intraperitoneally in 0.2-0.3 ml *per* animal for a minimum 2 hours sleeping time. Anaesthesia was maintained to the end of experiment with

additional Zoletil (0.1 ml, *i.p.*, 5.0 mg/kg), if necessary. Fur around the chest, abdomen and back areas of the animals was shaved to reduce scattering of the photoluminescence signal and localize it with maximal precision.

Then each mice was injected via lateral tail vein with 100 μ L 0.5 % wt. PA-UCNPs/PA dispersion (1mg/kg) (n = 10) in PBS, pH 7.2. Immediately after the injection, the animals were placed into the optical imaging system to evaluate the PA-UCNPs PL signal distribution time evolution. The detection of PL was carried out either from the ventral or back side of the animals.

Mice were sacrificed in 2 h after the injection of PA-UCNPs/ PA by using drug overdose method and necropsy was performed. Heart, lungs, liver, spleen, kidney were excised and fixed in 10% neutral buffered formalin for 48 h. After fixation, the excised organs were dehydrated in a graded series of alcohol, embedded in paraffin wax and cut into 5- μ m matched serial sections for conventional light microscopy histological examination and photoluminescence microscopy examination, respectively. The slices for histological study were stained with haematoxylin and eosin (H&E), following the conventional protocol, and examined using an upright light microscope Olympus BX51 (Olympus Optical, Tokyo, Japan) equipped with a SDU-252 digital camera (Spetstelektkhnik, Russia). The slices for PL measurements were left unstained. All samples were embedded in the polystyrene-based mounting media and covered by cover slips.

Conclusions

A new *in situ* method of synthesis of water-dispersible polymer particles impregnated with upconversion nanoparticles in the course of the acrolein polymerization was designed and demonstrated. The obtained uniform polymer particles were size-controllable in the range of 260 - 650 nm. The photoluminescence efficiency was found comparable to that of the state-of-the-art as-synthesised UCNPs, and immune to aqueous and physiological environments. The use of tetramethylammonium hydroxide both as a hydrophilizing agent (by way of displacing capping oleic acids) and initiator of the polymerization represented the key enabling step. The peculiarity of polymerization in the presence of UCNPs, consisted of precipitation and template method formation polymer particles, provided deep burying of UCNPs into polymer matrix. The feasibility of biomedical applications was demonstrated on the example of *in vivo* optical imaging of hybrid PA-UCNP particle distribution in a whole animal using a home-built epi-luminescence imaging system.

Acknowledgments

This work was supported by the Russian Science Foundation grant No.14-13-01421 (in part of synthesis of polymer dispersions and their characterization), by the Government of the Russian Federation Contract No. 14.Z50.31.0022 (in part of optical bioimaging) and Russian Foundation for

Basic Research projects No. 13-04-40228-H (in part of biosamples). The authors are grateful to Drs A.P. Popov, A.V. Bykov and L. Liang for carrying out TEM imaging of our samples, to T. Rudenko for the assistance in slices preparation for histology.

References

- 1 U. Resch-Genger, M. Grabolle, S. Cavaliere-Jaricot, R. Nitschke and T. Nann, *Nat. Methods*, 2008, **5**, 763.
- 2 S. Lee, E.J. Cha, K. Park, S.Y. Lee, J.K. Hong, I.C. Sun, S.Y. Kim, K. Choi and I.C. Kwon, *Angew. Chem.*, 2008, **47**, 2804.
- 3 Q. Zhao, M.X. Yu, L.X. Shi, S.J. Liu, C.Y. Li, M. Shi, Z.G. Zhou, C.H. Huang and F. Y. Li, *Organometallics*, 2010, **29**, 1085.
- 4 J. Mona, J.S. Tu, T.Y. Kang, C.Y. Tsai, E. Perevedentseva and C.L. Cheng, *Dia. & Rel. Mat.*, 2012, **24**, 134.
- 5 A. Nadort, V.K.A. Sreenivasan, Z. Song, E.A. Grebenik, A.V. Nechaev, V.A. Semchishen, V.Y. Panchenko and A.V. Zvyagin, *PLoS ONE*, 2013, **8**, e63292.
- 6 C. Bouzigues, T. Gacoin and A. Alexandrou, *ACS Nano*, 2011, **5**, 8488.
- 7 F. Auzel, *Chem. Rev.*, 2004, **104**, 139.
- 8 E.V. Khaydukov, V.A. Semchishen, V.N. Seminogov, A.V. Nechaev and A.V. Zvyagin, *Biomed. Opt. Express*, 2014, **5**, 1952.
- 9 C.T. Xu, N. Svensson, J. Axelsson, P. Svenmarker and G. Somesfalean, *Appl. Phys. Lett.*, 2008, **93**, 171103.
- 10 F. Wang and X.G. Liu., *Chem. Soc. Rev.*, 2009, **38**, 976.
- 11 J.C.G. Bunzli, *Chem. Rev.*, 2010, **110**, 2729.
- 12 M. Wang, G. Abbineni, A. Clevenger, C. Mao and S. Xu, *Nanomedicine: Nanotechnology, Biology, and Medicine*, 2011, **7**, 710.
- 13 Z. Chen, H. Chen, H. Hu, M. Yu and F. Li, *J. Am. Chem. Soc.*, 2008, **130**, 3023.
- 14 J.C. Boyer, M.P. Manseau, J.I. Murray and F.C.J.M. Veggel, *Langmuir*, 2010, **26**, 1157.
- 15 E.A. Grebenik, A. Nadort, A.N. Generalova, A.V. Nechaev, V.K.A. Sreenivasan, E.V. Khaydukov, V.A. Semchishen, A.P. Popov, V.I. Sokolov, A.S. Akhmanov, V.P. Zubov, D.V. Klinov, V.Y. Panchenko, S.M. Deyev and A.V. Zvyagin, *J. Biomed. Opt.*, 2013, **18**, 076004.
- 16 M. An, J. Cui, Q. He and L. Wang, *J. Mater. Chem. B*, 2013, **1**, 1333.
- 17 H. Zhang, Y. Li, I.A. Ivanov, Y. Qu, Y. Huang and X. Duan, *Angew. Chem.*, 2010, **49**, 2865.
- 18 Q. Liu, M. Chen, Y. Sun, G. Chen, T. Yang, Y. Gao, X. Zhang and F. Li, *Biomaterials*, 2011, **32**, 8243.
- 19 Z.Q. Li and Y. Zhang, *Angew. Chem.*, 2006, **45**, 7732.
- 20 A. Gnach and A. Bednarkiewicz, *Nano Today*, 2012, **7**, 532
- 21 M. Han, X. Gao, J.Z. Su and S. Nie, *Nat. Biotechnol.*, 2001, **19**, 631.
- 22 F. Yan, J. Li, J. Zhang, F. Liu and W. Yang, *J. Nanopart. Res.*, 2009, **11**, 289.

- 23 E. Dzunuzovic, K. Jeremica and J. M. Nedeljkovic, *Eur. Polymer J.*, 2007, **43**, 3719.
- 24 A.N. Generalova, S.V. Sizova, T.A. Zdobnova, M.M. Zarifullina, M.V. Artemyev, A.V. Baranov, V.A. Oleinikov, V.P. Zubov and S.M. Deyev, *Nanomedicine (London, U.K.)*, 2011, **6**, 195.
- 25 W. Sheng, S. Kim, J. Lee, S.W. Kim, K. Jensen and M.G. Bawendi, *Langmuir*, 2006, **22**, 3782.
- 26 S. Margel and E. Wiesel, *J. Polymer Sci. Polym. Chem. Ed.*, 1984, **22**, 145.
- 27 A.N. Generalova, M.M. Zarifullina, E.V. Lankina, S.V. Sizova, M.V. Artemyev, V.P. Zubov and V.A. Oleinikov, *J. Colloid and Interf. Sci.*, 2011, **357**, 265.
- 28 G. Chen, H. Qiu, P.N. Prasad and X. Chen, *Chem. Rev.*, 2014, **114**, 5161.
- 29 N. Bogdan, F. Vetrone, G.A. Ozin and J.A. Capobianco, *Nano Lett.*, 2011, **11**, 835.
- 30 F. Yan, J. Li, J. Zhang, F. Liu and W. Yang, *J. Nanopart. Res.*, 2009, **11**, 289.
- 31 A.L. Willis, N.J. Turro and S. O'Brien, *Chem. Mater.*, 2005, **17**, 5970.
- 32 *Reactivity, Mechanism and Structure in Polymer Chemistry*, ed. A.D. Jenkins and A Ledwith, J. Wiley & Sons, New York, 1974, pp. 645.
- 33 A. Ouasri, A. Rhandour, M.C. Dhamelincourt, P. Dhamelincourt and A. Mazzah, *Spectrochimica Acta*, 2002, **58**, 2779.
- 34 R.M. Silverstein and F.X. Webster, in *Spectrometric Identification of Organic Compounds*, John Wiley & Sons, New York, 6th edn, 1998, pp. 655.
- 35 A. Rembaum, M. Chang and J. Richards, *J. Polymer Sci., Polym. Chem. Ed.*, 1984, **22**, 609.
- 36 S. Slomkowski, *Prog. Polym. Sci.*, 1998, **23**, 815.
- 37 *Surfactants and Polymers in Aqueous Solution*, ed. K. Holmberg, B. Jonsson, B. Kronberg, and B. Lindman, J. Wiley & Sons, New York, 2nd edn, 2002, pp. 547.
- 38 S. Polowinski, in *Encyclopedia of Polymer Science and Technology*, J. Wiley & Sons, New York, 2003, pp.151.
- 39 G.D. Luker and K.E. Luker, *J. Nucl. Med.*, 2008, **49**, 1.